Alexandria Engineering Journal (2016) xxx, xxx–xxx

HOSTED BY

ELSEVIER

Alexandria University

Alexandria Engineering Journal

www.elsevier.com/locate/aej
www.sciencedirect.com

ORIGINAL ARTICLE

Irreversibility analysis for reactive third-grade fluid flow and heat transfer with convective wall cooling

Samuel O. Adesanya [a,*], J.A. Falade [b], Srinivas Jangili [c], O. Anwar Bég [d]

[a] *Department of Mathematical Sciences, Redeemer's University, Ede, Nigeria*
[b] *Department of Physical Sciences, Redeemer's University, Ede, Nigeria*
[c] *Department of Mathematics, National Institute of Technology Meghalaya, Shillong, India*
[d] *Spray Research Group, Petroleum and Gas Engineering Division, Room G77, Newton Building, School of Computing, Science and Engineering (CSE), University of Salford, M54WT, UK*

Received 2 July 2016; revised 19 September 2016; accepted 24 September 2016

KEYWORDS

Entropy generation;
Convective cooling;
Reactive third grade viscoelastic fluid;
Irreversibility ratio;
Thermal polymer processing

Abstract Inherent irreversibility in the flow of a reactive third grade fluid though a channel with convective heating is examined. It is well known that heat dissipated from the exothermic chemical reaction passes through fluid in an irreversible manner and as a result entropy is generated continuously within the channel. Analytical solutions of the resulting dimensionless nonlinear boundary-value-problems arising from the governing equations were obtained by using perturbation method. These solutions are utilized to obtain the entropy generation rate and Bejan number for the system. The influence of various important parameters on the entropy generation rate and Bejan number are shown graphically and discussed accordingly.

1. Introduction

Studies related to reactive viscous incompressible fluid flow through a channel are important in several manufacturing, energy and petrochemical applications. Chemical reactions may be extremely sophisticated in viscoelastic polymer flows as described by Kamal and Ryan [1]. Lactic acid production is another example of non-Newtonian reactive flow [2,3]. A comprehensive description of the many complex polymers arising in different systems has been provided quite recently by Halley and George [4]. In [4] the importance of improving mathematical models to describe transport phenomena more accurately has also been emphasized. A number of researchers in recent years have therefore investigated both analytically and numerically chemical reaction phenomena in non-Newtonian processing systems. For instance, Makinde [5–7] studied the flow and stability of combustible fluid using a powerful and rapidly convergent analytical approximant. Chinyoka [8] employed Direct Numerical Simulation (DNS) to study two-dimensional Oldroyd-B viscoelastic flow with Arrhenius kinetics and thermal convection. Bég et al. [9] employed a spectral quasilinearization numerical method to investigate the flow of combustible gel propellant in a hybrid rocket chamber with Newtonian cooling. They utilized the third grade Rivlin-Ericksen ("differential" fluid) model for viscoelasticity and validated solutions carefully with the

* Corresponding author.
E-mail addresses: adesanyas@run.edu.ng (S.O. Adesanya), j.srinivasnit@gmail.com (S. Jangili).

Peer review under responsibility of Faculty of Engineering, Alexandria University.

http://dx.doi.org/10.1016/j.aej.2016.09.017

variational iteration method (VIM). Further studies of strongly exothermic fluid flows in various geometries are documented in Refs. [10–16].

In recent years, entropy generation modeling has also become an active area of thermal engineering sciences since heat passes through a fluid in an irreversible manner and there is an obvious change in entropy of the fluid particles. This is attributable to the temperature difference in the fluid particle which will lead to a random or disordered motion of the fluid particles. Evidently, this will minimize the efficiency of the system. Motivated by the fact that many thermal processes occur at extremely high temperature, the principal objective of this analysis was to examine the thermal performance of the channel flow problem studied earlier by Makinde [5]. This is necessary to measure the efficiency of the setup since increased entropy depletes the energy level of the system. The approach here follows the second law of thermodynamics that is based on the original pioneering work of Bejan [17] which has revolutionized thermal optimization of engineering processes and subsequently used by Adesanya and Makinde [18], Adesanya and Falade [19], Adesanya and Makinde [20] and Adesanya et al. [21] for non-Newtonian liquids. Pakdemirli and Yilbas [22] considered the third grade fluid model with Vogel viscosity to study the entropy generation analysis in a pipe. They showed that different viscosity parameters may either increase or decrease the entropy generation number. Hooman et al. [23] obtained numerical solutions for entropy effects on forced convection flow in a channel. More recent works on entropy generation analysis for various flow configurations is documented in [24–31].

The plan of study is as follows: in Section 2, the mathematical formulation (reactive non-Newtonian fluid dynamics and heat transfer) of the problem is presented. In Section 3 perturbative series solutions are presented for the non-dimensional boundary value problem while in Section 4, the entropy generation analysis is described. In Section 5, graphical results and interpretation are provided. Section 6 concludes the paper.

2. Mathematical reactive non-Newtonian thermofluid model

Steady-state laminar flow of a chemically-reactive fluid between two rigid horizontal parallel plates containing an isotropic, homogenous porous medium saturated with the fluid is considered. The exothermic chemical reaction is simulated following Arrhenius kinetics and a third grade non-Newtonian Rivlin-Ericksen ("differential" fluid) model is implemented to simulate the viscoelastic effects. The channel depth is $2a$. The fluid flow is induced by a constant applied axial pressure gradient and is hydrodynamically and thermally fully developed. The physical model is illustrated below in Fig. 1. The equations governing the transport, following Makinde [5] are as follows:

$$-\frac{dP}{dx}+\mu\frac{d^2u}{dy'^2}+6\beta_3\frac{d^2u}{dy'^2}\left(\frac{du}{dy'}\right)^2=0 \tag{1}$$

$$k\frac{d^2T}{dy'^2}+\mu\left(\frac{du}{dy'}\right)^2\left(1+\frac{2\beta_3}{\mu}\left(\frac{du}{dy'}\right)^2\right)+QC_0Ae^{-\frac{E}{RT}}=0 \tag{2}$$

The appropriate boundary conditions imposed are as follows:

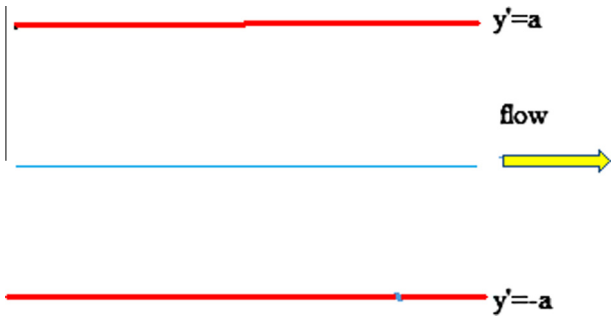

Figure 1 Viscoelastic reactive channel flow domain.

$$\text{At}\quad y'=+a: u=0;\ \frac{dT}{dy'}=-h(T-T_0) \tag{3}$$

$$\text{At}\quad y'=0: \frac{du}{dy'}=\frac{dT}{dy'}=0 \tag{4}$$

Here u is the fluid velocity, T is the fluid temperature, h is the heat transfer coefficient, k is the thermal conductivity of the material, Q is the heat of reaction, A is the rate constant, C_0 is the initial concentration of the reactant species, R is the universal gas constant, β_3 is the material coefficient, E is the activation energy, P is the modified fluid pressure and μ is the dynamic viscosity of the non-Newtonian fluid. The following dimensionless quantities and parameters are deployed to obtain the non-dimensional form of the governing equations:

$$\begin{aligned}
&\theta=\frac{E(T-T_a)}{RT_a^2},\ y=\frac{y'}{a},\ \lambda=\frac{QEAa^2C_0e^{-\frac{E}{RT_a}}}{RT_a^2k},\\
&w=\frac{u}{UG},\ Bi=\frac{ha}{k},\\
&G=-\frac{a^2}{\mu U}\frac{dP}{dx},\ m=\frac{\mu G^2U^2e^{\frac{E}{RT_a}}}{QAa^2C_0},\ \in=\frac{RT_a}{E},\\
&\gamma=\frac{\beta_3U^2G^2}{\mu a^2},\ N_s=\frac{a^2E^2E_G}{kR^2T_a^2}
\end{aligned} \tag{5}$$

Here U is the fluid characteristic velocity, T_a is the ambient temperature, θ denotes non-dimensional temperature, y is dimensionless channel width (depth), w is dimensionless axial velocity, Bi is the Biot number, G is the non-dimensional pressure gradient parameter, γ is the dimensionless non-Newtonian (viscoelastic material) parameter within which β_3 is the third grade viscoelastic fluid material parameter [32], λ represents the Frank-Kamenetskii chemical kinetic parameter, m is the viscous heating parameter and $\in$ is activation energy parameter.

In view of Eq. (5), the dimensionless boundary-value problem assumes the form:

$$1+\frac{d^2w}{dy^2}+6\gamma\frac{d^2w}{dy^2}\left(\frac{dw}{dy}\right)^2=0 \tag{6}$$

$$\frac{d^2\theta}{dy'^2}+\lambda\left[e^{\frac{\theta}{1+\in\theta}}+m\left(\frac{dw}{dy}\right)^2\left(1+2\gamma\left(\frac{dw}{dy}\right)^2\right)\right]=0 \tag{7}$$

The corresponding normalized boundary conditions become the following:

Please cite this article in press as: S.O. Adesanya et al., Irreversibility analysis for reactive third-grade fluid flow and heat transfer with convective wall cooling, Alexandria Eng. J. (2016), http://dx.doi.org/10.1016/j.aej.2016.09.017

$$\left.\begin{array}{ll} w=0,\ \frac{d\theta}{dy}=-Bi\theta & \text{on } y=1 \\ \frac{dw}{dy}=0,\ \frac{d\theta}{dy}=0 & \text{on } y=0 \end{array}\right\} \tag{8}$$

3. Methods of solution

3.1. Perturbation technique

Following [5], to obtain the analytical solution of Eqs. (6)–(8), we assume a perturbative series solution of the form:

$$w=\sum_{n=0}^{\infty}u_n\gamma^n,\ \ \theta=\sum_{n=0}^{\infty}\theta_n\lambda^n \tag{9}$$

where $0<\gamma\ll 1$ and $0<\lambda\ll 1$ are assumed small parameters. Substituting (9) in (7) and (8) and equating coefficients, we get the following:

$$\left.\begin{array}{l} \sum_{n=0}^{\infty}u_n=a_0-\int_0^y\int_0^y\{1+6\gamma A_n\}dYdY \\ \sum_{n=0}^{\infty}\theta_n=b_0-\lambda\int_0^y\int_0^y\left\{B_n+m\left(\frac{d}{dY}\sum_{n=0}^{\infty}u_n\right)^2\left(1+2\gamma\left(\frac{d}{dY}\sum_{n=0}^{\infty}u_n\right)^2\right)\right\}dYdY \end{array}\right\} \tag{17}$$

$$\left.\begin{array}{ll} \frac{d^2w_0}{dy^2}+1=0; & \frac{dw_0}{dy}(0)=0=w_0(1) \\ \frac{d^2w_1}{dy^2}+6\frac{d^2w_0}{dy^2}\left(\frac{dw_0}{dy}\right)^2=0; & \frac{dw_1}{dy}(0)=0=w_1(1) \\ \frac{d^2w_2}{dy^2}+12\frac{d^2w_0}{dy^2}\left(\frac{dw_0}{dy}\right)\left(\frac{dw_1}{dy}\right)+6\frac{d^2w_1}{dy^2}\left(\frac{dw_0}{dy}\right)^2=0 & \frac{dw_2}{dy}(0)=0=w_2(1) \\ \cdots & \end{array}\right\} \tag{10}$$

together with

$$\left.\begin{array}{ll} \frac{d^2\theta_0}{dy^2}=0; & \frac{d\theta_0}{dy}(0)=0,\ \frac{d\theta_0}{dy}(1)+Bi\theta_0(1)=0 \\ \frac{d^2\theta_1}{dy^2}+\left[e^{\frac{\theta_0}{1+\varepsilon\theta_0}}+m\left(\frac{dw}{dy}\right)^2\left(1+2\gamma\left(\frac{dw}{dy}\right)^2\right)\right]=0; & \frac{d\theta_1}{dy}(0)=0,\ \frac{d\theta_1}{dy}(1)+Bi\theta_1(1)=0 \\ \frac{d^2\theta_2}{dy^2}+\frac{\theta_1}{(1+\varepsilon\theta_1)^2}e^{\frac{\theta_0}{1+\varepsilon\theta_0}}=0; & \frac{d\theta_2}{dy}(0)=0,\ \frac{d\theta_2}{dy}(1)+Bi\theta_2(1)=0 \\ \cdots & \end{array}\right\} \tag{11}$$

Eqs. (10) and (11) are coded in the **DifferentialSolve** algorithm in a symbolic package - Mathematica. This gives the solutions as partial sums:

$$w=\sum_{n=0}^{M}u_n\gamma^n,\ \ \theta=\sum_{n=0}^{M}\theta_n\lambda^n \tag{12}$$

where M is the point of truncation for the series solution. Due to large output of the symbolic solutions only graphical results are presented in Section 5 and the series expansions are omitted for brevity.

3.2. Adomian Decomposition Method (ADM)

To validate the accuracy of the solutions obtained by regular perturbation above, we need to validate the solution using another rapidly converging semi-numerical method [33]. To implement this method, the dimensionless boundary-valued-problems (6)–(8) are integrated as follows:

$$u(y)=a_0-\int_0^y\int_0^y\left\{1+6\gamma\frac{d^2u}{dY^2}\left(\frac{du}{dY}\right)^2\right\}dYdY \tag{13}$$

$$\theta(y)=b_0-\lambda\int_0^y\int_0^y\left\{e^{\frac{\theta}{1+\varepsilon\theta}}+m\left(\frac{du}{dY}\right)^2\left(1+2\gamma\left(\frac{du}{dY}\right)^2\right)\right\}dYdY \tag{14}$$

The solutions of the integral Eqs. (13) and (14) are assumed in the form:

$$u=\sum_{n=0}^{\infty}u_n,\ \ \theta=\sum_{n=0}^{\infty}\theta_n \tag{15}$$

We first identify the nonlinear terms as follows:

$$A=\frac{d^2u}{dY^2}\left(\frac{du}{dY}\right)^2,\quad B=e^{\frac{\theta}{1+\varepsilon\theta}} \tag{16}$$

Using (15) in (13) and (14) we obtain

In view of (17), each term of the series can be obtained using

$$\left.\begin{array}{l} u_0(y)=a_0-\int_0^y\int_0^y(1)dydy \\ u_{n+1}(y)=-\int_0^y\int_0^y(6\gamma A_n)dydy \quad n\geqslant 0 \end{array}\right\} \tag{18}$$

and

$$\left.\begin{array}{l} \theta_0(y)=0 \\ \theta_1(y)=b_0-\lambda\int_0^y\int_0^y\left\{B_0+m\left(\frac{du}{dY}\right)^2\left(1+2\gamma\left(\frac{du}{dY}\right)^2\right)\right\}dYdY \\ \theta_{n+1}(y)=-\lambda\int_0^y\int_0^y(B_n)dYdY \qquad n\geqslant 1 \end{array}\right\} \tag{19}$$

Noting (16), the Adomian polynomials for the nonlinear terms are computed as follows:

$$\left.\begin{array}{l} A_0=\frac{d^2u_0}{dY^2}\left(\frac{du_0}{dY}\right)^2 \\ A_1=2\frac{d^2u_0}{dY^2}\left(\frac{du_0}{dY}\right)\left(\frac{du_1}{dY}\right)+\frac{d^2u_1}{dY^2}\left(\frac{du_0}{dY}\right)^2 \\ A_2=\frac{d^2u_0}{dY^2}\left(\frac{du_1}{dY}\right)^2+2\frac{d^2u_0}{dY^2}\left(\frac{du_0}{dY}\right)\left(\frac{du_2}{dY}\right)+2\frac{d^2u_1}{dY^2}\left(\frac{du_0}{dY}\right)\left(\frac{du_1}{dY}\right)+\frac{d^2u_2}{dY^2}\left(\frac{du_0}{dY}\right)^2 \\ \cdots \end{array}\right\} \tag{20}$$

$$\left.\begin{array}{l} B_0=e^{\frac{\theta_0}{1+\varepsilon\theta_0}} \\ B_1=\frac{\theta_1}{(1+\varepsilon\theta_1)^2}e^{\frac{\theta_0}{1+\varepsilon\theta_0}} \\ B_2=\frac{\left\{(1-2\varepsilon-2\varepsilon^2\theta_0)\theta_1^2+2(1+\varepsilon\theta_0^2\theta_2)\right\}}{2(1+\varepsilon\theta_1)^4}e^{\frac{\theta_0}{1+\varepsilon\theta_0}} \\ \cdots \end{array}\right\} \tag{21}$$

Table 1 Convergence of solutions when $M = 3, \in = 0.1 = m = \lambda, Bi = 10,\ \gamma = 0.01$.

y	$w_{Perturbation}$	w_{ADM}	*Abs Error*	$\theta_{Perturbation}$	θ_{ADM}	*Abs Error*
−1	0	1.7130E−17	1.71E−17	0.0108030	0.0108057	2.6886E−06
−0.75	0.215486	0.215486	0	0.0343656	0.0343748	9.18258E−06
−0.5	0.370497	0.370497	0	0.0511111	0.0511258	1.46827E−05
−0.25	0.463957	0.463957	0	0.0611240	0.0611424	1.83873E−05
0	0.495188	0.495188	0	0.0644559	0.0644756	1.96960E−05
0.25	0.463957	0.463957	0	0.0611240	0.0611424	1.83873E−05
0.5	0.370497	0.370497	0	0.0511111	0.0511258	1.46827E−06
0.75	0.215486	0.215486	0	0.0343656	0.0343748	9.18258E−06
1	0	1.7130E−17	1.71E−17	0.0108030	0.0108057	2.68862E−06

The following partial sum

$$u = \sum_{n=0}^{M} u_n,\ \ \theta = \sum_{n=0}^{M} \theta_n \tag{22}$$

are used to evaluate the unknown constants and consequently the approximate solutions. Eqs. (18)–(22) are carefully coded in Mathematica software giving out huge symbolic solutions. Convergence of the two solution methods is shown in Table 1.

4. Entropy generation analysis

The heat transfer process within the channel is irreversible [18]. Then the random motion of the fluid particles within the flow channel and heat transfer encourages entropy production. Mathematically, the equation for the total entropy generation arising from heat transfer and fluid friction irreversibilities can then be written as

$$E_G = \frac{k}{T_a^2}\left(\frac{dT}{dy'}\right)^2 + \frac{\mu}{T_a}\left(\frac{du'}{dy'}\right)^2\left(\mu + 2\beta_3\left(\frac{du'}{dy'}\right)^2\right) \tag{23}$$

Using the aforementioned dimensionless quantities and parameters, as defined in Eq. (5), the equation for the dimensionless form of (13), emerges in due course, as follows:

$$N_S = \left(\frac{d\theta}{dy}\right)^2 + \frac{\lambda m}{\in}\left(\frac{dw}{dy}\right)^2\left(1 + 2\gamma\left(\frac{dw}{dy}\right)^2\right) \tag{24}$$

Now, substituting Eq. (12) into Eq. (14), the entropy production rate for the flow in the channel can be computed.

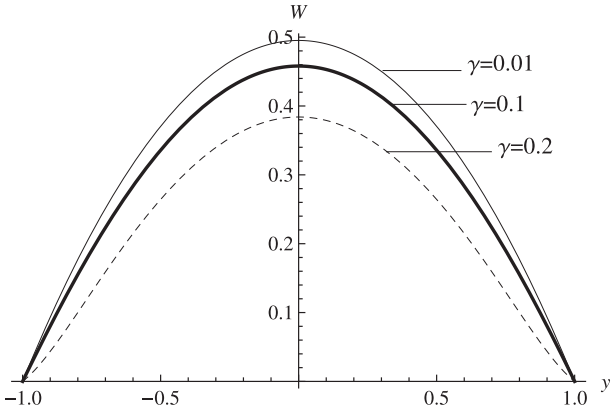

Figure 2 Velocity profile at different values of Frank-Kamenetskii parameter.

Using (14), we get N_1, N_2 represent heat transfer and fluid friction irreversibilities respectively:

$$N_1 = \left(\frac{d\theta}{dy}\right)^2,\ \ N_2 = \frac{\lambda m}{\in}\left(\frac{dw}{dy}\right)^2\left(1 + 2\gamma\left(\frac{dw}{dy}\right)^2\right) \tag{25}$$

Next, we get the Bejan number (Be) as follows:

$$Be = \frac{N_1}{N_S} = \frac{N_1}{N_1 + N_2} = \frac{1}{1 + \Phi},\quad \Phi = \frac{N_2}{N_1} \tag{26}$$

The graphical results for Ns are shown in Figs. 2–6 and those corresponding to Be and Φ are illustrated in Figs. 7–11.

5. Results and interpretation

In this section, the graphical results associated with Eqs. (22) and (23) are presented for various values of the flow parameters.

Fig. 2 describes the effect of Frank-Kamenetskii parameter on velocity field. As this parameter increases, the velocity decreases. Fig. 3 displays the variation of Frank-Kamenetskii parameter on temperature distribution. Increased Frank-Kamenetskii parameter values lead to increase in the reaction and viscous heating source terms and therefore increases the temperature.

Fig. 4 illustrates the entropy generation rate at various values of the Frank-Kamenetskii parameter (λ). As seen from the plot, elevating the Frank-Kamenetskii parameter encourages entropy generation in the flow channel. This is physically true since internal heat generation increases with the increasing concentration of the reagents. The exothermic chemical interactions encourage the rate of heat transfer from the combustion zone to the cool wall. In addition, the heat is transferred through the fluid has melting effect on the fluid viscosity, and this means that inter-particle collision will be encourage; thus, more heat is being generated by viscous interaction of the fluid particles. Therefore, concentration of the reagent is one factor to be monitored to achieve the best result.

Fig. 5 depicts the effect of third grade material parameter (γ) on the entropy generation in the channel. From the graph, entropy production in the fluid layer closer to the walls decreases as the non-Newtonian material parameter increases. This is because as the third grade material effect increases, the fluid becomes more viscoelastic as a result of stronger bonding forces between the fluid particles in the laminar flow. Also, the heat released due to exothermic chemical reaction is absorbed to excite the fluid particles. Hence entropy generation must be on the decrease as presented in the graph. The downward trend

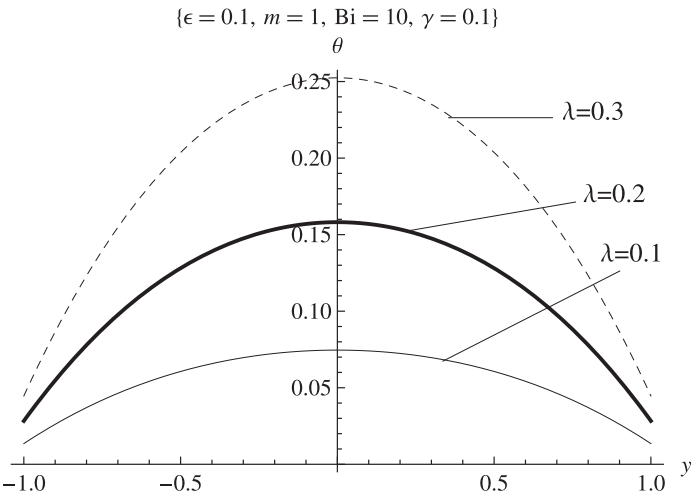

Figure 3 Temperature profile at different values of Frank-Kamenetskii parameter.

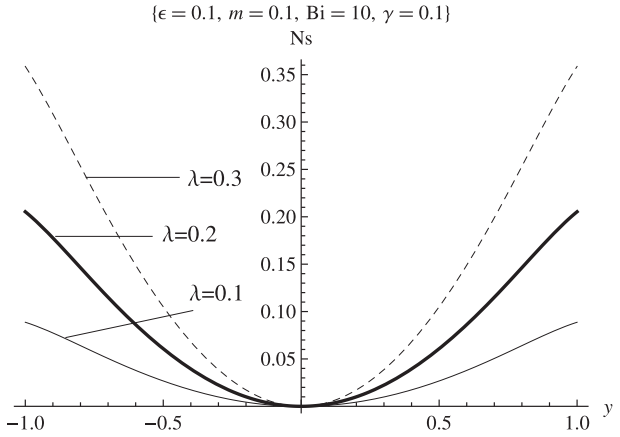

Figure 4 Entropy generation at different values of Frank-Kamenetskii parameter.

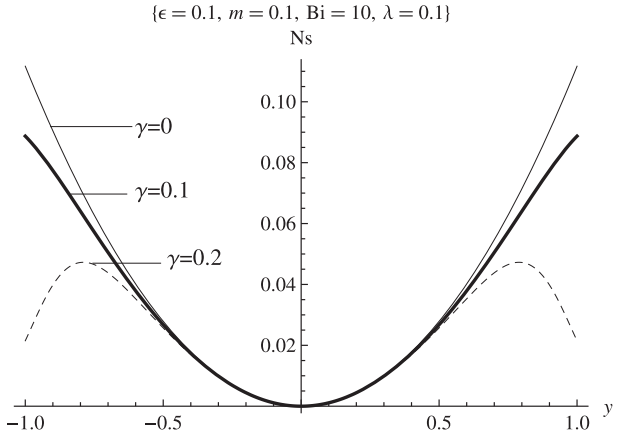

Figure 5 Entropy generation at different values of third grade material effect.

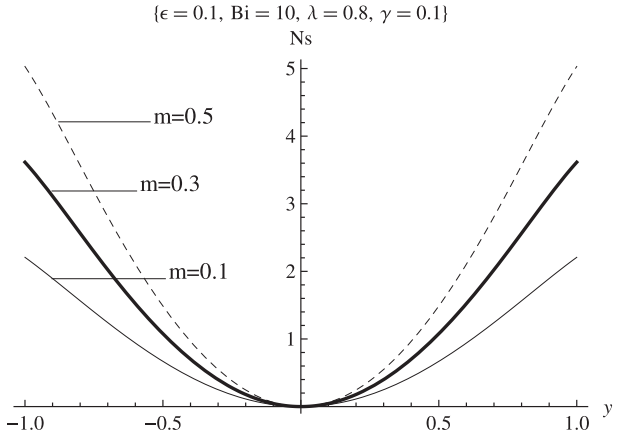

Figure 6 Entropy generation at different values of viscous heating parameter.

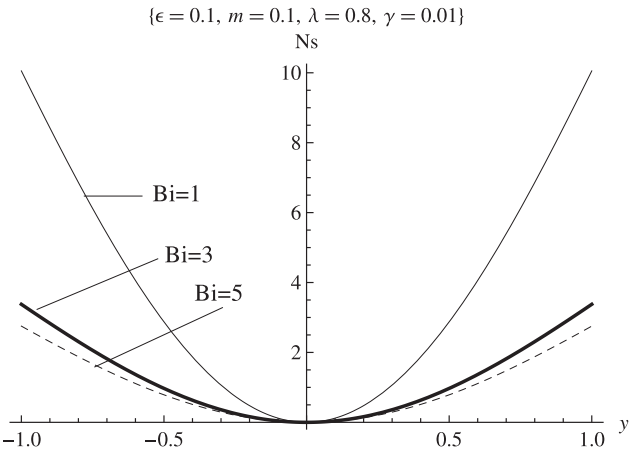

Figure 7 Entropy generation at different values of Biot number.

observed here is due to the imbalance between the nonlinear heat and the linear convective cooling at the walls as the third grade material parameter increases.

In Fig. 6, the influence of viscous heating parameter (m) on the entropy generation rate within the flow channel is presented. It is clear that an increase in the viscous heating param-

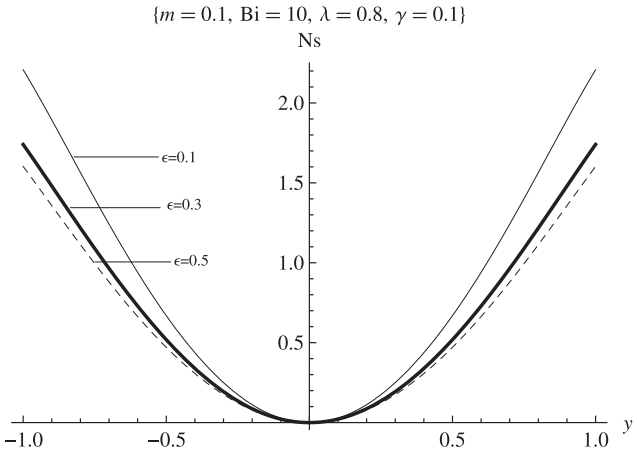

Figure 8 Entropy generation at different values of activation energy parameter.

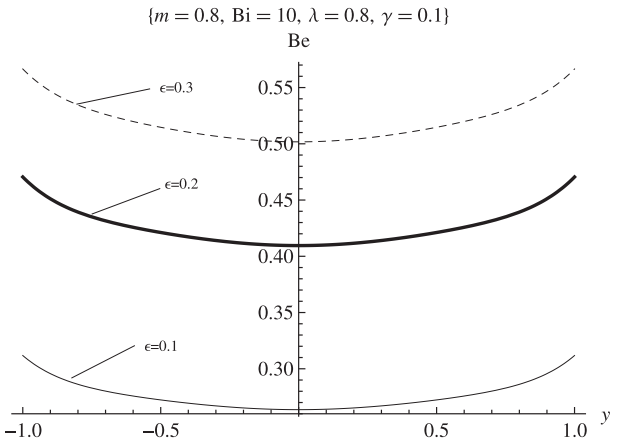

Figure 9 Bejan number at different values of activation energy parameter.

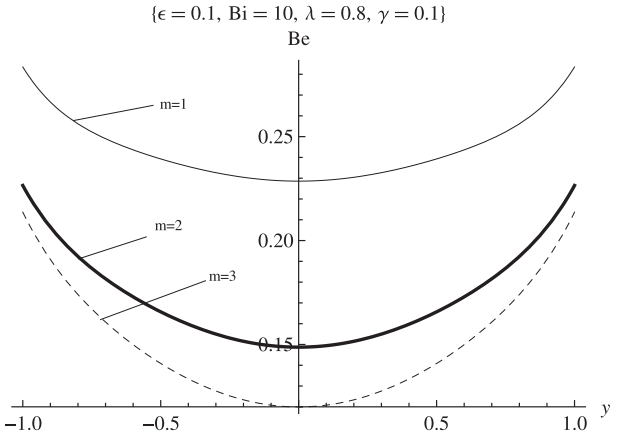

Figure 10 Bejan number at different values of viscous heating parameter.

eter enhances the entropy production. This is correct in view of the fact that more and more heat is liberated from inter-particle collisions; in other words, kinetic energy generates heat energy since it is an additional heat source.

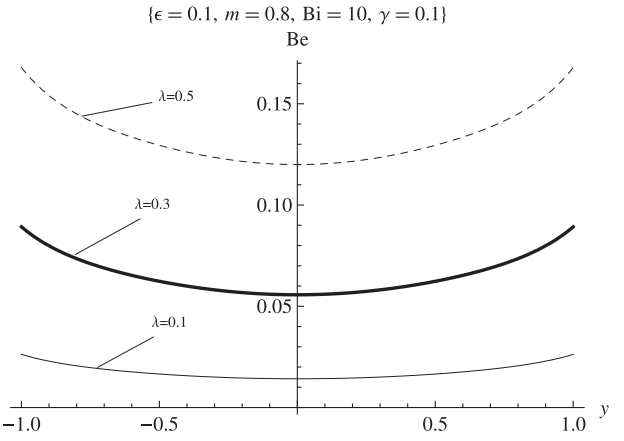

Figure 11 Bejan number at different values of Frank-Kamenetskii parameter.

Fig. 7 depicts the entropy generation rate as the symmetric Biot number increases at the walls. As shown in the graph the entropy generation rate decreases with an increase in the convective cooling parameter. This is due to the irreversible heat flow from the surface of hot walls to the ambient, in a manner that satisfies the Newtonian cooling law. This results in a minimization of the entropy in the fluid region close to the cool walls. Biot numbers considered are much greater than 0.1 i.e. this corresponds to the "thermally thick" scenario as elaborated by Prasad et al. [34] and Bég et al. [35]. The case where $Bi < 0.1$ is known as the "thermally-thin" scenario and is not relevant to polymeric flows since heat conduction inside the body is much faster than the heat convection away from its surface implying that temperature gradients are negligible inside the body. The Biot number ($Bi = ha/k$) is directly proportional to the convection heat transfer coefficient at the channel wall and inversely proportional to thermal conductivity, for a given channel width. Lower thermal conductivity is associated therefore with higher Biot numbers and significant cooling.

Fig. 8 displays the effect of the activation energy parameter ($\in$) on the entropy generation rate. As seen from the plot an increase in the activation energy parameter is observed to lower the entropy generation rate within the flow channel. This arises since a rise in the fluid activation energy parameter corresponds to a decrease in the fluid activation energy. Hence, the higher the activation energy parameter, the lower the temperature. Therefore this reduction in temperature is expected to discourage entropy generation within the channel. Similarly an increase in the activation energy parameter physically means an associated decrease in the fluid friction due to a rise in fluid viscosity as shown in Eq. (15) (the viscoelastic parameter, γ, featuring in Eq. (15) is inversely proportional to the dynamic viscosity).

Fig. 9 demonstrates that with increasing activation energy parameter ($\in$), Bejan number is consistently enhanced across the channel span. Evidently, as the irreversibility due to fluid friction continues to decrease, the Bejan number tends to be elevated and eventually will attain unity value. This is physically correct since increase in activation energy parameter as shown in earlier implies decreased activation energy and reduced fluid viscosity. When this happens, heat transfer is expected to dominate over fluid friction irreversibility.

Please cite this article in press as: S.O. Adesanya et al., Irreversibility analysis for reactive third-grade fluid flow and heat transfer with convective wall cooling, Alexandria Eng. J. (2016), http://dx.doi.org/10.1016/j.aej.2016.09.017

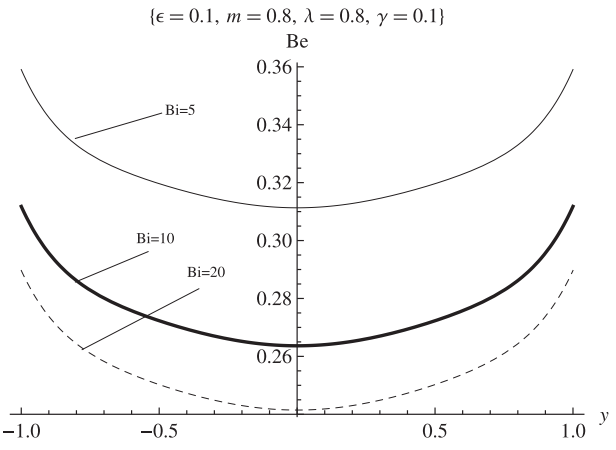

Figure 12 Bejan number at different values of Biot number.

Fig. 10 illustrates the variation in Bejan number across the channel with viscous heating parameter (m). As viscous heating increases, more heat is generated within the flow channel due to increased frictional interactions within the moving fluid layers and hence fluid friction irreversibility dominates over heat transfer irreversibility in the channel.

Fig. 11 shows the response in Bejan number with various values of the Frank-Kamenetskii parameter (λ). As seen from the graph, an increase in the Frank-Kamenetskii parameter leads to huge increase in the heat transfer irreversibility due to the exothermic nature of the chemical reaction. Therefore, heat transfer dominates over fluid friction irreversibility as the Frank-Kamenetskii parameter increases, i.e. as the chemical kinetic effect intensifies.

Fig. 12 depicts the evolution in Bejan number with a variation in Biot number. An increase in Biot number is shown to strongly reduce Bejan number. The result shows that heat transfer to the wall decreases as the convective cooling at the walls intensifies. Hence irreversibility due to fluid friction (viscous dissipation) dominates over heat transfer as the Biot number increases.

6. Conclusion

In the present analysis, we have examined the heat irreversibility in the exothermically reactive flow of a third grade fluid through a vertical channel with convective cooling at the walls. The irreversibility analysis has been conducted using the second law of thermodynamics. The dimensionless momentum and heat conservation equations have been solved by perturbation method. The velocity and temperature solutions have been used to compute the entropy generation number (Ns) and Bejan number (Be). The present investigation has shown that for the thermally-thick scenario:

(i) an increase in both viscous heating and Frank-Kamenetskii parameter needs to be monitored since they contribute significantly to destruction of the thermo-fluid system while third grade material effect, Biot number and activation energy discourage entropy profile.

(ii) an increase in the fluid activation energy and Frank-Kamenetskii was seen to encourage the dominance of heat transfer irreversibility over fluid friction. On the other hand, increasing values of the Biot number and viscous heating parameter encourages fluid friction irreversibility over heat transfer irreversibility in the flow channel.

The present analysis has neglected time-dependent effects, which will be addressed soon.

References

[1] M.R. Kamal, M.E. Ryan, Reactive polymer processing: techniques and trends, Adv. Polymer Technol. 4 (1984) 323–348.
[2] S.S. Bapat, C.P. Aichele, K.A. High, Development of a sustainable process for the production of polymer grade lactic acid, Sust. Chem. Process. 2 (2014) 1–8.
[3] R. Datta, M. Henry, Lactic acid: recent advances in products, processes and technologies – a review, J. Chem. Technol. Biotechnol. 81 (2006) 1119–1129.
[4] P.J. Halley, G.A. George, Chemo-rheology of Polymers: From Fundamental Principles to Reactive Processing, Cambridge University Press, UK, 2009.
[5] O.D. Makinde, On thermal stability of a reactive third-grade fluid in a channel with convective cooling at the walls, Appl. Math. Comput. 213 (2009) 170–176.
[6] O.D. Makinde, On steady flow of a reactive variable viscosity fluid in a cylindrical pipe with an isothermal wall, Int. J. Numer. Methods Heat Fluid Flow 17 (2) (2007) 187–194.
[7] O.D. Makinde, Thermal ignition in a reactive viscous flow through a channel filled with a porous medium, ASME J. Heat Transfer 128 (2006) 601–604.
[8] T. Chinyoka, Two-dimensional flow of chemically reactive viscoelastic fluids with or without the influence of thermal convection, Commun. Nonlinear Sci. Numer. Simul. 16 (2011) 1387–1395.
[9] O.A. Bég, S.S. Motsa, M.N. Islam, M. Lockwood, Pseudo-spectral and variational iteration simulation of exothermically-reacting Rivlin-Ericksen viscoelastic flow and heat transfer in a rocket propulsion duct, Comput. Therm. Sci. 6 (2014) 91–102.
[10] S.O. Ajadi, A note on the thermal stability of a reactive non-Newtonian flow in a cylindrical pipe, Int. Commun. Heat Mass Transfer 36 (2009) 63–68.
[11] S.S. Okoya, Disappearance of criticality for reactive third-grade fluid with Reynold's model viscosity in a flat channel, Int. J. Non-Linear Mech. 46 (2011) 1110–1115.
[12] S.S. Okoya, On the transition for a generalized Couette flow of a reactive third-grade fluid with viscous dissipation, Int. Commun. Heat Mass Transfer 35 (2008) 188–196.
[13] S.S. Okoya, Thermal stability for a reactive viscous flow in a slab, Mech. Res. Commun. 33 (2006) 728–733.
[14] S.S. Okoya, Criticality and transition for a steady reactive plane Couette flow of a viscous fluid, Mech. Res. Commun. 34 (2007) 130–135.
[15] T. Hayat, R. Ellahi, F.M. Mahomed, Exact solutions for thin film flow of a third grade fluid down an inclined plane, Chaos, Solitons Fractals 38 (2008) 1336–1341.
[16] M. Danish, Shashi Kumar, Surendra Kumar, Exact analytical solutions for the Poiseuille and Couette-Poiseuille flow of third grade fluid between parallel plates, Commun. Nonlinear Sci. Numer. Simul. 17 (2012) 1089–1097.
[17] A. Bejan, Entropy Generation through Heat and Fluid Flow, Wiley, New York, 1982.

[18] S.O. Adesanya, O.D. Makinde, Irreversibility analysis in a couple stress film flow along an inclined heated plate with adiabatic free surface, Physica A 432 (2015) 222–229.
[19] S.O. Adesanya, J.A. Falade, Thermodynamics analysis of hydromagnetic third grade fluid flow through a channel filled with porous medium, Alexandria Eng. J. 54 (2015) 615–622.
[20] S.O. Adesanya, O.D. Makinde, Entropy generation in couple stress fluid flow through porous channel with fluid slippage, Int. J. Exergy 15 (2014) 344–362.
[21] S.O. Adesanya, S.O. Kareem, J.A. Falade, S.A. Arekete, Entropy generation analysis for a reactive couple stress fluid flow through a channel saturated with porous material, Energy 93 (2016) 1239–1245.
[22] M. Pakdemirli, B.S. Yilbas, Entropy generation for pipe low of a third grade fluid with Vogel model viscosity, Int. J. Non-Linear Mech. 41 (3) (2006) 432–437.
[23] K. Hooman, F. Hooman, S.R. Mohebpour, Entropy generation for forced convection in a porous channel with isoflux or isothermal walls, Int. J. Exergy 5 (1) (2008) 78–96.
[24] D.S. Chauhan, V. Kumar, Entropy analysis for third-grade fluid flow with temperature-dependent viscosity in annulus partially filled with porous medium, Theor. Appl. Mech. 40 (3) (2013) 441–464.
[25] S. Das, R.N. Jana, Entropy generation due to MHD flow in a porous channel with Navier slip, Ain Shams Eng. J. 5 (2014) 575–584.
[26] J. Srinivas, J.V. Ramana Murthy, Second law analysis of the flow of two immiscible micropolar fluids between two porous beds, J. Eng. Thermophys. 25 (1) (2016) 126–142.
[27] D. Srinivasacharya, K. Hima Bindu, Entropy generation in a micropolar fluid flow through an inclined channel, Alexandria Eng. J. (2016), http://dx.doi.org/10.1016/j.aej.2016.02.027 (in press).
[28] J. Srinivas, J.V. Ramana Murthy, A.J. Chamkha, Analysis of entropy generation in an inclined channel flow containing two immiscible micropolar fluids using HAM, Int. J. Numer. Meth. Heat Fluid Flow 23 (2016) 1027–1049.
[29] G. Nagaraju, J. Srinivas, J.V. Ramana Murthy, A.M. Rashad, Entropy generation analysis of the MHD flow of couple stress fluid between two concentric rotating cylinders with porous lining, Heat Transfer Asian Res. (2016), http://dx.doi.org/10.1002/htj.21214 (in press).
[30] N.S. Akbar, M. Shoaib, D. Tripathi, S. Bhushan, O.A. Bég, Analytical approach for entropy generation and heat transfer analysis of CNT-nanofluids through ciliated porous medium, J. Hydrodyn. B (2016) (in press).
[31] S. Jangili, N. Gajjela, O. Anwar Beg, Mathematical modeling of entropy generation in magnetized micropolar flow between co-rotating cylinders with internal heat generation, Alexandria Eng. J. 55 (2016) 1969–1982.
[32] O.A. Bég, H.S. Takhar, R. Bhargava, S. Rawat, V.R. Prasad, Numerical study of heat transfer of a third grade viscoelastic fluid in non-Darcian porous media with thermophysical effects, Phys. Scr. 77 (2008) 1–11.
[33] A.M. Siddiqui, M. Hameed, B.M. Siddiqui, Q.K. Ghori, Use of Adomian decomposition method in the study of parallel plate flow of a third grade fluid, Commun. Nonlinear Sci. Numer. Simul. 15 (2010) 2388–2399.
[34] V.R. Prasad, S. Abdul Gaffar, E. Keshava Reddy, O.A. Bég, Computational study of non-Newtonian thermal convection from a vertical porous plate in a non-Darcy porous medium with Biot number effects, J. Porous Media 17 (7) (2014) 601–622.
[35] O.A. Bég, M.J. Uddin, M.M. Rashidi, N. Kavyani, Double-diffusive radiative magnetic mixed convective slip flow with Biot and Richardson number effects, J. Eng. Thermophy. 23 (2014) 79–97.

Please cite this article in press as: S.O. Adesanya et al., Irreversibility analysis for reactive third-grade fluid flow and heat transfer with convective wall cooling, Alexandria Eng. J. (2016), http://dx.doi.org/10.1016/j.aej.2016.09.017